Continuous Estimation of Acute Changes in Preload Using Epicardially Attached Accelerometers

Magnus Reinsfelt Krogh, Per Steinar Halvorsen, Ole-Johannes H. N. Grymyr, Jacob Bergsland, Ole Jakob Elle, Erik Fosse, and Espen W. Remme

Abstract*—*Objective: **A miniaturized accelerometer can be incorporated in temporary pacemaker leads which are routinely attached to the epicardium during cardiac surgery and provide continuous monitoring of cardiac motion during and following surgery. We tested if such a sensor could be used to assess volume status, which is essential in hemodynamically unstable patients.** ***Methods:*** **An accelerometer was attached to the epicardium of 9 pigs and recordings performed during baseline, fluid loading, and phlebotomy in a closed chest condition. Alterations in left ventricular (LV) preload alter myocardial tension which affects the frequency of myocardial acceleration associated with the first heart sound (f_{S1}). The accuracy of f_{S1} as an estimate of preload was evaluated using sonomicrometry measured end-diastolic volume (EDV_{SONO}). Standard clinical estimates of global end-diastolic volume using pulse index continuous cardiac output (PiCCO) measurements ($GEDV_{PiCCO}$) and pulmonary artery occlusion pressure (PAOP) were obtained for comparison. The diagnostic accuracy of identifying fluid responsiveness was analyzed for f_{S1}, stroke volume variation (SVV_{PiCCO}), pulse pressure variation (PPV_{PiCCO}), $GEDV_{PiCCO}$, and PAOP.** ***Results:*** **Changes in f_{S1} correlated well to changes in EDV_{SONO} ($r^2 = 0.81$, 95%CI: [0.68, 0.89]), as did $GEDV_{PiCCO}$ ($r^2 = 0.59$, 95%CI: [0.36, 0.76]) and PAOP ($r^2 = 0.36$, 95%CI: [0.01, 0.73]). The diagnostic accuracy [95%CI] in identifying fluid responsiveness was 0.79 [0.66, 0.94] for f_{S1}, 0.72 [0.57, 0.86] for SVV_{PiCCO}, and 0.63 (0.44, 0.82) for PAOP.** ***Conclusion:*** **An epicardially placed accelerometer can assess changes in preload in real-time.** ***Significance:*** **This novel method can facilitate continuous monitoring of the volemic status in open-heart surgery patients and help guiding fluid resuscitation.**

***Index Terms*—Accelerometer, first heart sound, fluid responsiveness, heart wall vibration, hemodynamic monitoring, PiCCO, preload.**

I. Introduction

TEMPORARY pace leads are routinely placed on the heart during open heart surgery. Miniaturized accelerometers can be combined with temporary pace leads providing a possibility to extract more valuable clinical information of hemodynamic status of the patient without any added surgical procedure. Such information can include heart wall motion and thus ventricular function. We have previously demonstrated this concept of monitoring cardiac function in real time, including automatic detection of myocardial ischemia and evaluation of inotropic state [1]–[4]. In cardiac surgery, assessments of intravascular volume state and preload are essential as volume expansion usually is the first line of therapy in a bleeding patient postoperatively. An accelerometer, incorporated in the temporary pace leads, may potentially also be used for such assessment and for guiding fluid therapy during hemodynamic instability. Such a device could entail a temporary pace wire with accelerometer incorporated connected to a bedside monitor that continuously estimates the left ventricular volume. It is accepted that central venous pressure poorly predicts left ventricular preload status and response to a fluid challenge [5]. Despite this fact, the central venous pressure remains the routine method for continuous assessment of the volemic state in cardiac surgery. Other methods using arterial waveform to estimate pulse-pressure and stroke volume variations are only applicable in mechanical ventilated patients and have not gained wide acceptance in cardiac surgery [6]. Thermodilution based methods and echocardiography are tools to guide hemodynamic optimization but can only be used intermittently.

The acceleration signal from the myocardium exhibits several high frequency oscillations or vibrations during the various phases of the cardiac cycle. Previous studies of these signals have investigated relationship between peak endocardial acceleration associated with the first heart sound and contractility, or how the frequency of the first heart sound changes during early systole [7], [8]. However, estimating preload using frequency analysis of myocardial vibrations has not been explored.

Manuscript received July 12, 2020; accepted August 21, 2020. Date of publication August 31, 2020; date of current version June 18, 2021. This work was supported by South-Eastern Norway Regional Health Authority Project 2014076. *(Corresponding author: Espen Remme.)*

Magnus Reinsfelt Krogh and Ole Jakob Elle are with the Intervention Centre, Oslo University Hospital and also with Department of Informatics, University of Oslo.

Per Steinar Halvorsen, Ole-Johannes H. N. Grymyr, Jacob Bergsland, and Erik Fosse are with the Intervention Centre, Oslo University Hospital.

Espen W. Remme is with the Intervention Centre, Oslo University Hospital, 0450 Oslo, Norway, and also with the Institute for Surgical Research, Oslo University Hospital, 0450 Oslo, Norway (e-mail: espen.remme@medisin.uio.no).

Digital Object Identifier 10.1109/TBME.2020.3020358

Loading and unloading the left ventricle affect the myocardial tension at end diastole and beginning of systole. Changes in myocardial tension may alter the vibrations of the heart induced by valve events in a similar manner known from the physics of vibrating strings where the frequency is a function of tension as well as length and density. We therefore hypothesized that this analogy could be transferred to the myocardium and that the frequency of the measured myocardial vibration was proportional to the tension in the myocardium at end diastole and hence preload. We further hypothesized that this measure, based on data from a single epicardially placed accelerometer, could be used to identify states of fluid responsiveness.

To test our hypotheses, as a proof of concept, we used an animal model with changing intravascular volume by fluid administration and phlebotomy. We compared the accelerometer-based indices with gold standard continuous volume measurements using sonomicrometry, in addition to clinically standard measurements by PiCCO and pulmonary artery catheters.

II. Materials and Methods

A. Animal Preparation

The animal protocol was approved by the Norwegian Food Safety Authority [project ID: 9303] and carried out in accordance with Norwegian regulations concerning use of animals in experiments [FOR-2015-06-18-761]. We used 12 NOROC pigs (4 male) and average weight 44 kg ($\pm$2 kg SD.). The animals were premedicated with an intramuscular injection of ketamine 20 mg/kg, azaperone 3 mg/kg and atropine 0.02 mg/kg. Anesthesia was induced by intravenous thiopental 2-3 mg/kg and morphine 0.5–1 mg/kg. Immediately after induction of anesthesia, tracheotomy was performed and anesthesia upheld by inhalation (isoflurane 1-2%) and morphine 0.50-1.0 mg/kg/h, adjusted by the animal's autonomous stress response. A Leon respirator was used for ventilation and gas monitoring with inspired oxygen fraction of 0.35. The animals were monitored by 3-lead electrocardiogram (ECG) placed on the chest (reference lead on the abdomen), peripheral oxygen saturation (SpO2), temperature and diuresis. The internal and external jugular veins were cannulated for introduction of a central venous pressure catheter and pulmonary artery catheter (Edwards Lifesciences Corporation, Irvine, CA, USA). The carotid arteries were cannulated to introduce two 5-Fr Millar pressure catheters into the left ventricle (LV) and aortic outlet. A PiCCO catheter (Pulsion, Munich, Germany) was introduced via a femoral artery.

After introduction of anesthesia and hemodynamic monitoring, sternotomy was performed, and the pericardial sack was split from apex to base exposing the heart. To measure the LV volume, we placed sonomicrometry crystals sub-endocardially in a long axis pair (apex to anterior base), and short axis pair (equatorial, postero-lateral to antero-septal). From these two pairs the continuous volume could be estimated using the formula $V = \frac{\pi}{6} W^2 H$, where W and H were the distance between the short axis pair and long axis pair, respectively [9].

To measure the myocardial vibrations, we developed a sensor assembly comprising an inertial sensor (MPU9250, InvenSense Inc, San Jose, CA, USA) which was placed in the anterior LV apical region. A detailed description of the accelerometer assembly was described in our previous study [10]. In short: we mounted the sensor, and necessary components, on a small printed circuit board (PCB) (5 $\times$ 10 mm), which was coated with epoxy and enclosed with a shrinking tube for easier suturing to the heart, as shown in Fig. 1 top panels. A thin, flexible wire was soldered to the PCB which enabled powering (5 V) and I2C data communication. The acquisition unit (Cardiaccs AS, Oslo, Norway) comprised an USB to I2C converter and was connected to a computer that ran a specially designed LabView (National Instruments, Austin, TX, USA) application for data recording. The acquisition unit also comprised an analog to digital converter which was used to record ECG. Data were recorded at 700 S/s, with an operational range of $\pm$ 8 G. No calibration other than factory calibration was done on the accelerometer. Fig. 1, bottom panel, shows the instrumentation of the sensor.

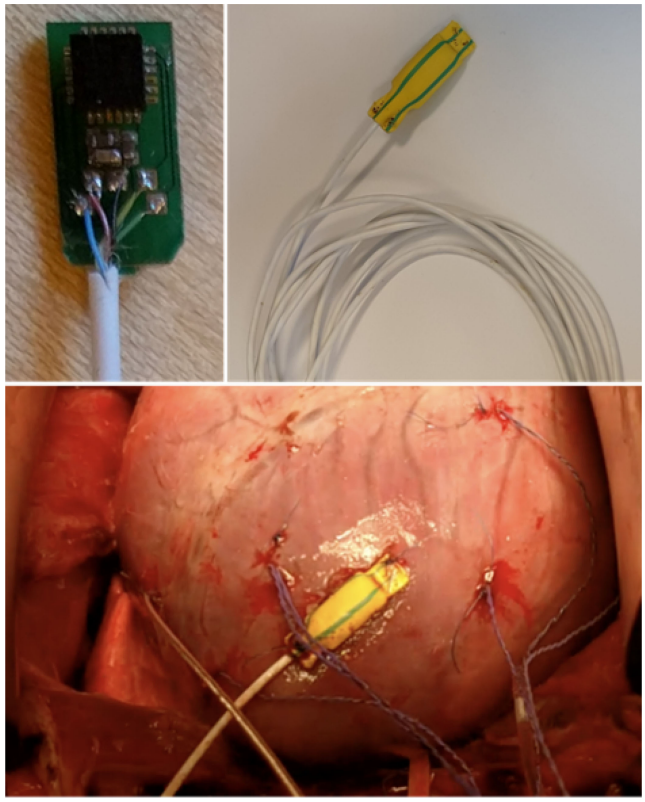

Fig. 1. Pictures showing the accelerometer sensor used in this study. Top left: the printed circuit board with added components. Top right: the sensor assembly with wire and shrinking tube mounted. Bottom: the sensor placed in the anterior, apical region of the left ventricle.

Lastly, the thorax was closed by suturing sternum and skin. The intervention protocol was started after a 30 minutes stabilization period following instrumentation.

In order to reduce the number of animals, the same animals were also included in another study [10]. The protocol of the other study required two additional sonomicrometry crystals placed on each side of the accelerometer. The interventions of that study were performed subsequently to the experimental protocol described in this study, and therefore did not affect the results presented. In addition to the twelve animals included in this study, there were three animals that underwent the other protocol first and suffered fatal complications before any data

was gathered for this study. They are hence not reported in the total number of animals used for this study.

B. Experimental Protocol

After a baseline recording, preload was increased by volume loading of 250 ml 0.9% NaCl solution in intervals until a 10% increase in end diastolic volume (EDV) was observed in the sonomicrometric volume trace. Recordings were obtained between each interval of loading. To decrease preload, blood was drained from the central venous catheter into heparinized bags in 250 ml or 500 ml intervals, in between recordings, until a 10% decrease in EDV from baseline was achieved.

C. Hemodynamic Measurements

Pulmonary artery occlusion pressure (PAOP) was recorded as an index of LV filling pressure. Using sonomicrometry, end diastolic volume (EDV_{SONO}), stroke volume (SV_{SONO}), cardiac output (CO_{SONO}), and stroke volume variation (SVV_{SONO}) were recorded as reference values. From the PiCCO recordings, cardiac output (CO_{PiCCO}), global end-diastolic volume ($GEDV_{PiCCO}$), stroke volume (SV_{PiCCO}), stroke volume variation (SVV_{PiCCO}), and pulse pressure variation (PPV_{PiCCO}) were extracted for comparison with sonomicrometry and accelerometer derived values. All these measurements were performed in between the loading and unloading steps as described in the preceding section.

D. Accelerometer Measures of Myocardial Vibrations and Preload

Preload is defined as wall stress at end diastole (ED) which by Laplace's law depends on wall thickness (w), pressure (P), and radius (r) of the ventricle. Mersenne's law states that the frequency of a vibrating string can be expressed as a function of its length (L), density (μ) and tension (T):

$$f = \frac{1}{2L}\sqrt{\frac{T}{\mu}} \tag{1}$$

If we transfer this concept to the myocardium and assume that the size and density of the myocardium is constant during the time of measuring, then the frequency of the measured vibration in the myocardium at ED is proportional to the square root of the tension in the myocardium, i.e. preload. High frequency myocardial vibration would indicate higher preload and thereby increased volemic state, and conversely, low frequency would indicate a hypovolemic ventricle. At the time of the first heart sound following mitral valve closure, rapid vibrations can be seen in the accelerometer recordings (Fig. 2). The frequency of these vibrations was analyzed and correlated with alterations in preload as described below.

E. Accelerometer Signal Processing and Analysis

1) Pre-Processing: We used the Python programming language (version 3.6.9, Python Software Foundation) for all signal pre-processing. From the recordings we chose data from at least 3 respiration cycles, to ensure that the values were unaffected by changes due to respiration. End diastole was defined as the ECG Q-wave, and end systole was defined as minimum LV dP/dt.

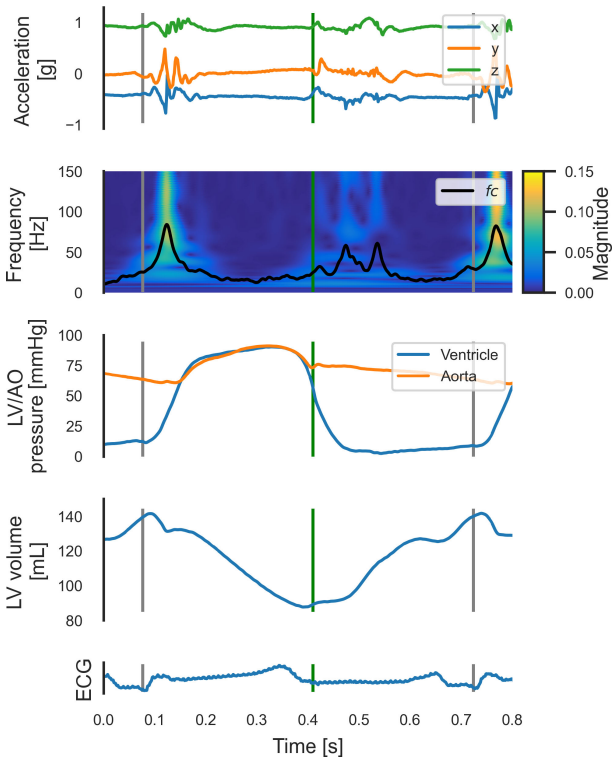

Fig. 2. Recordings from an animal with a 3-axis accelerometer sutured to the epicardium. Top panel shows raw acceleration. The second panel shows the frequency spectrum over time (wavelet scalogram, only shown for the x-axis for illustration purposes). The black trace in the frequency spectrum (f_c) represents the center frequency for each time point. Additional panels show left ventricular pressure (LVP), aortic pressure (AOP), LV volume, and ECG. Vertical grey line indicate time of Q in ECG and green line time of minimum LV dP/dt.

The raw accelerometer signals were filtered using a 5th order Butterworth band-pass filter with cut off frequencies at 20 Hz and 250 Hz to remove high frequency noise and unwanted effects of respiration and heart rate on the frequency analysis. Since the accelerometer senses in three spatial directions (x, y, and z), we performed the frequency analysis on each axis individually and reported the average of these. This measure will therefore be independent of the orientation of the sensor placement on the heart.

2) Wavelet Analysis of Accelerometer Signal: Wavelet analysis was used to analyze the frequency components of the acceleration associated with the first heart sound using MATLAB's (The MathWorks, Natick, MA, USA) function CWT using the analytic Morlet wavelet, with a symmetry parameter of 3 and a time-bandwidth product of 60. This CWT function converts the scales to a frequency output using pseudo-frequencies approximation. Wavelet analysis was chosen above Fast Fourier Transform analysis to preserve the temporal resolution in the signal, as the first heart sound occurs in a brief moment of time relative to the sensor's sampling frequency. The continuous wavelet transform produces a spectrogram containing the power of each frequency component in a signal over time, as shown in Fig. 3. The color represents the magnitude of the particular frequency components. To extract the dominant frequency at any given time, we calculated the weighted average frequency for each time point (f_C), also known as the center frequency.

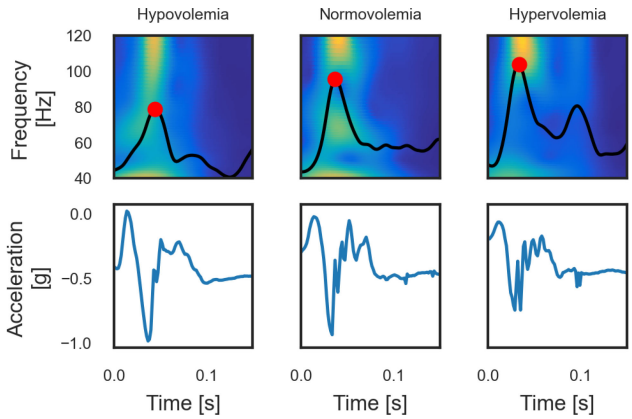

Fig. 3. Graphs showing cropped outtakes from the frequency spectrogram (upper panels) and raw acceleration traces (lower panels) during the first 150 ms after end diastole (ED) for hypovolemia (left panels), normovolemia (middle panels), and hypervolemia (right panels). The black traces represent the center frequency (f_C) for each timepoint and the red circle represents the point of maximum frequency (f_{S1}) within the time window. The graphs show only x-axis acceleration, for illustration purposes.

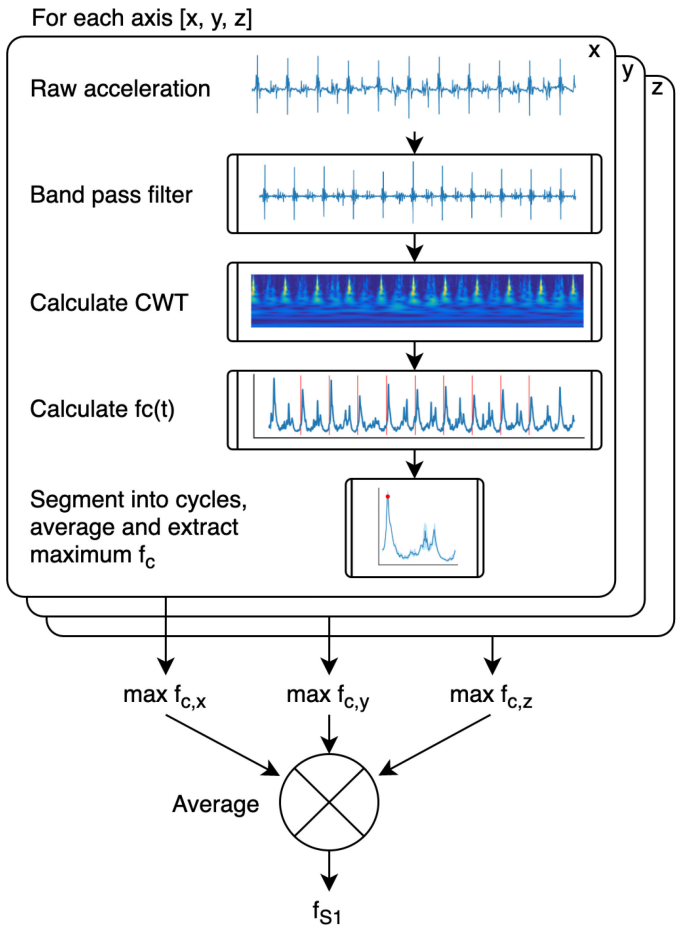

Fig. 4. Flowchart describing the signal pre-processing procedure. For each axis, the raw acceleration trace is filtered to remove high, and low frequency noise. The continuous wavelet transform (CWT) is calculated from the resulting trace. The center frequency trace ($f_c(t)$) is calculated from the CWT. The $f_c(t)$ is then segmented into cycles based on r-peaks. The segments are averaged, and the maximum $f_c(t)$ is extracted. f_{S1} was determined as the average $max f_c$ of the three axes.

According to the hypothesis, increased preload would shift the frequencies upward and hence elevate f_C. To investigate such frequency shifts, we extracted the maximum value of the center frequency (f_{S1}) during the first heart sound (S1) within 0.03 and 0.1 s after ED. This window was chosen to exclude high frequency noise that was sometimes observed just prior to ED. The f_C trace oscillated with respiration, having lower values during expiration than inspiration. Since the hypothesis was that the overall frequency would be elevated, we chose to remove the respiration variations by averaging the center frequency trace for all heart cycles spanning the recording of at least 3 respiration cycles. The f_{S1} was then calculated from this average cycle. A correlation analysis was then performed to assess the relationship between the myocardial frequency and EDV_{SONO}. A diagram of the signal processing step is shown in Fig. 4.

F. Preload Estimation Accuracy

In this study we used changes in EDV_{SONO} as an index for changes in preload. Linear regression and Bland-Altman analyses were performed to determine the accuracy of f_{S1}, $GEDV_{PiCCO}$, and PAOP referenced to EDV_{SONO}. In order to perform a comparison of how well different measurements with different units (Hz, ml, and mmHg) correlated with EDV_{SONO} (ml), we also assessed and correlated the relative percentage change in the parameter values from baseline.

G. Correlation Between Stroke Volume and Estimated Preload Parameters

Together with a measure of cardiac function, the estimated preload parameter using the novel accelerometer method, may be used to continuously monitor the patient's Frank-Starling relation. To show how the novel method compares to the different modalities ability to estimate the Frank-Starling curve we correlated the estimated preload parameters with SV_{SONO}.

H. Fluid Responsiveness

The threshold value for stroke volume variation (SVV) in defining fluid responsiveness was set as 11.6% according to the review study by Marik*et al.* [6] Using SVV_{SONO} as reference, the accuracy of the accelerometer based method to correctly identify the fluid responsiveness was investigated and compared with PiCCO based measurements and pulmonary artery occlusion pressure. A receiver operating characteristics (ROC) analysis was performed, and the area under the ROC curve (AUC) for each method was used to assess and compare their accuracies.

I. Statistical Analyses

All statistical analyses were performed using R (v3.5.1) [11]. No statistical power calculation was conducted prior to the study as it was intended as a proof of concept. The sample size was therefore based on the available data. A total of 12 experiments were conducted. Three experiments were excluded due to either equipment malfunction ($n = 2$) or fatal bleeding

TABLE I
HEMODYNAMIC VARIABLES AT BASELINE AND THE VOLUME INTERVENTION EXTREMES ($n = 8$)

		Baseline	Maximum fluid loading	Maximum fluid unloading
Sonomicrometry	EDV [mL]	112 (27)	121 (30)*	94 (23)*
	SV [mL]	42 (10)	50 (14)*	32 (9.6)*
	CO [L/min]	4.5 (1.7)	5.3 (2.3)*	3.6 (1.4)*
	EF [%]	38 (6.3)	42 (7.1)*	34 (6.1)*
	SW [mL·mmHg]	2840 (1246)	3727 (1473)*	1586 (837)*
	SVV [%]	16 (7.5)	9.6 (4.0)*	24 (9.7)*
Accelerometer	$f_{S1}x$ [Hz]	83 (8.8)	89 (13)*	75 (7.2)*
	$f_{S1}y$ [Hz]	85 (11)	88 (11)	75 (8.6)*
	$f_{S1}z$ [Hz]	79 (12)	86 (14)*	71 (12)*
	$f_{S1}avg$ [Hz]	82 (8.7)	88 (8.4)*	74 (8.6)*
PiCCO	GEDV [mL]	588 (80)	624 (118)*	483 (69)*
	CO [L/min]	4.8 (1.1)	5.9 (1.3)*	4.2 (1.4)*
	SVV [%]	12 (4.1)	6.2 (1.3)*	15 (7.5)*
	PPV [%]	15 (6.3)	8.6 (3.8)*	24 (6.0)*
Hemodynamics	MAP [mmHg]	70 (15)	80 (15)*	53 (11)*
	CVP [mmHg]	11 (1.7)	14 (3.4)*	9.1 (1.8)*
	HR [bpm]	104 (31)	104 (29)	113 (32)
	SvO2 [%]	59 (9.6)	55 (7.1)	44 (12)*
	PAOP [mmHg]	13 (2.2)	16 (4.2)	12 (3.6)

Values reported as mean (SD). *: $p < 0.05$ vs baseline. EDV: end diastolic volume; SV: stroke volume; CO: cardiac output; EF: ejection fraction; SW: stroke work; SVV: stroke volume variation; f_{S1} [x,y,z,avg]: frequency of myocardial acceleration during the first heart sound; GEDV: global end-diastolic volume; PPV: pulse pressure variation; MAP: mean arterial pressure; CVP: central venous pressure; HR: heart rate; SvO2: venous oxygen saturation; PAOP: pulmonary artery occlusion pressure. One animal where unloading was performed before loading, did not reach a state of overloading, and was therefore excluded from this table.

due to left atrial rupture ($n = 1$). To test for significant effects of the interventions in Table I we used two-tailed Student's paired sample t-test. Normality of distributions was determined using Shapiro-Wilks test. To test differences in area under two receiver operating characteristic curves (AUC) we used DeLong's test [12]. Significance was determined as $p \leq 0.05$. No outliers have been excluded from the statistical tests. Values are reported as mean (SD) unless stated otherwise. The sample size in this study is relatively low and the statistical tests must therefore be considered with caution. We have therefore chosen to report the confidence intervals rather than rely on statistical tests where appropriate.

III. RESULTS

A. Hemodynamics

Hemodynamic values from baseline and the maximal and minimal volume loading conditions are reported in Table I. The EDV_{SONO} changed significantly both at maximum loading and maximum unloading. So did SV_{SONO}, CO_{SONO}, EF_{SONO}, SW_{SONO} and SVV_{SONO}. f_{S1}, measured using the accelerometer, showed a significant decrease for all axes (x, y, and z) in addition to the average, during maximum volume unloading. At maximum loading the f_{S1} showed a significant increase for x- and z-axes, as well as the average, but not for the y-axis. The PiCCO based parameters ($GEDV_{PiCCO}$, SV_{PiCCO}, CO_{PiCCO}, SVV_{PiCCO}, PPV_{PiCCO}) all showed a significant change during both unloading and loading. Pulmonary artery occlusion pressure did not significantly change for either extreme.

B. Preload Estimation Accuracy

Preload estimated by the frequency of myocardial acceleration (f_{S1}) showed a very strong average correlation to the reference EDV_{SONO}, as shown in Fig. 5A, when assessing each individual animal. This was comparable to the global end-diastolic volume ($GEDV_{PiCCO}$), shown in Fig. 5B, and the pulmonary artery occlusion pressure, shown in Fig. 5C. When pooling the data for all animals and looking at the relative change from baseline in the estimated preload parameters Δf_{S1} showed a strong correlation to the reference with an $r^2 = 0.81$ (95%CI: [0.68, 0.89]), as shown in Fig. 5D, while $\Delta GEDV_{PiCCO}$ (Fig. 5E) and ΔPAOP (Fig. 5F) had r^2 values of 0.59 (95%CI: [0.36, 0.76]) and 0.36 (95%CI: [0.01, 0.73]), respectively.

Relative changes in mean arterial pressure ΔMAP, and central venous pressure ΔCVP, had r^2 values of 0.78 (95%CI: [0.62, 0.88]) and 0.57 (95%CI: [0.34, 0.75]), respectively. The Bland-Altman analysis (Fig. 6) showed that the bias of Δf_{S1} compared to the ΔEDV was 1.0% with limits of agreement at -7.9 and 10.0%. The mean bias, and spread, for ΔGEDV was comparable to Δf_{S1}, having a value of 4.0% and limits of agreement at -13.6 and 21.5%.

C. Correlation Between Stroke Volume and Estimated Preload Parameters

The results from the linear regression analysis assessing the correlation between SV_{SONO} and the estimated preload parameters f_{S1}, $GEDV_{PiCCO}$, and PAOP are shown in Fig. 7. The average correlation coefficient for individual animals between SV_{SONO} and f_{S1} was comparable to $GEDV_{PiCCO}$ and PAOP. The pooled results, based on relative changes from baseline (Fig. 7, bottom row), showed that the correlation to stroke volume for f_{S1} ($r^2 = 0.72$, 95%CI: [0.55, 0.84]) was comparable to that of PAOP ($r^2 = 0.55$, 95%CI: [0.12, 0.83]) and $GEDV_{PiCCO}$ ($r^2 = 0.51$, 95%CI: [0.27, 0.71]).

D. Fluid Responsiveness

The results from the ROC analysis to identify the states of fluid responsiveness using f_{S1}, SVV_{PiCCO}, PPV_{PiCCO}, $GEDV_{PiCCO}$, PAOP, and heart rate are shown in Fig. 8 including the AUC values. The AUC-value for f_{S1} was comparable to SVV_{PiCCO}, PPV_{PiCCO}, $GEDV_{PiCCO}$, and PAOP. Heart rate had a significantly lower AUC than f_{S1} ($p = 0.01$). The sensitivity and specificity for f_{S1}, choosing the optimal cut-off value from the ROC analysis, was 87 and 67%, respectively. For SVV_{PiCCO}, PPV_{PiCCO}, $GEDV_{PiCCO}$, PAOP, and heart rate the sensitivities and specificities were, 81 and 60%; 70 and 60%; 56 and 71%; 55 and 64%; and 57 and 67%, respectively.

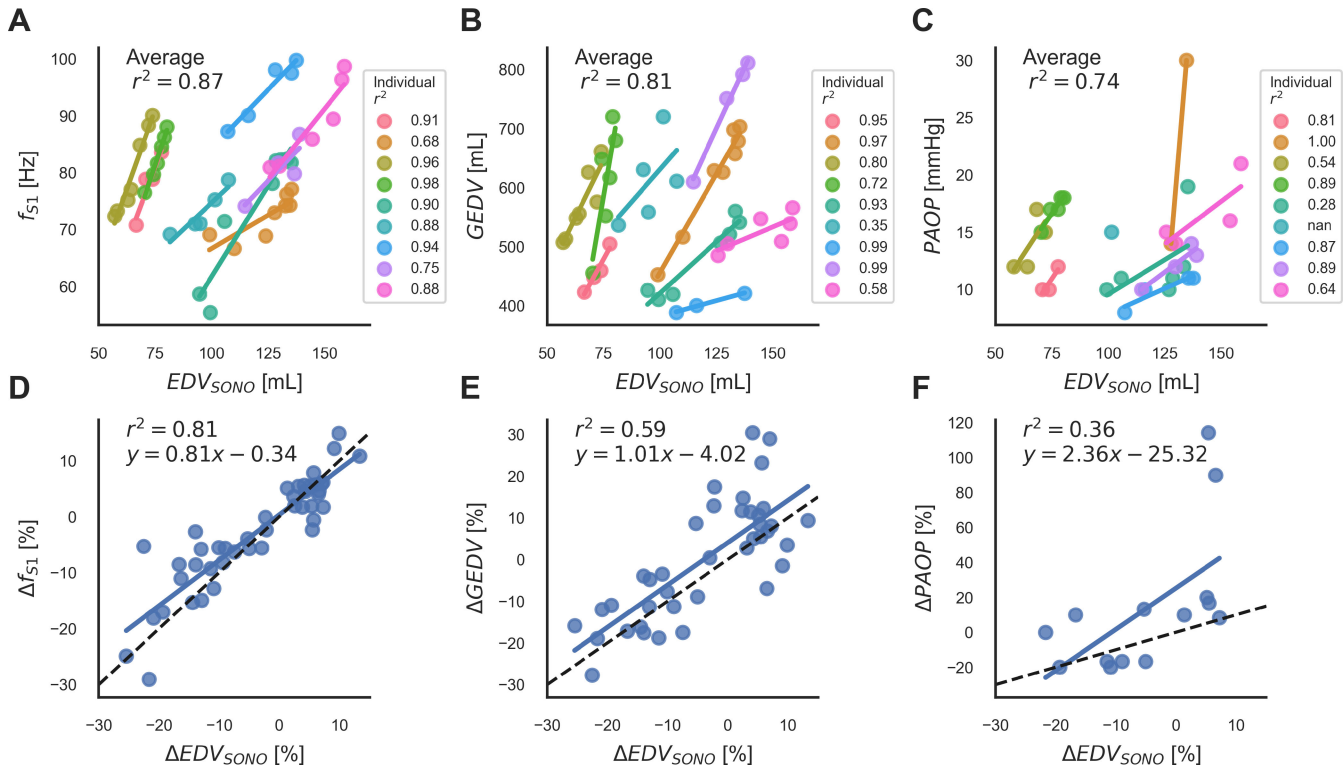

Fig. 5. Subplots A, B, and C show the correlation to EDV_{SONO} for f_{S1}, GEDV, and PAOP, respectively, for each individual animal. Subplots D, E, and F show the correlation to ΔEDV_{SONO} for Δf_{S1}, ΔGEDV, and ΔPAOP for data pooled from all experiments. Solid line signifies the regression line. Black, stippled line signifies $x = y$. f_{S1}: frequency of myocardial acceleration during the first heart sound. Δf_{S1}: relative change in f_{S1} from baseline. EDV_{SONO}: end-diastolic volume measured using sonomicrometry. ΔEDV_{SONO}: relative changes in EDV_{SONO}. GEDV: global end-diastolic volume measured using PiCCO. ΔGEDV: relative changes in GEDV. PAOP: pulmonary artery occlusion pressure. ΔPAOP: relative changes in PAOP.

IV. Discussion

In this study we have shown that relative changes in left ventricular preload can be measured by an accelerometer attached to the epicardium by assessing the changes in the frequency of myocardial acceleration during the first heart sound (f_{S1}). As EDV and myocardial stiffness increased, the frequency of the myocardial acceleration associated with the first heart sound also increased and vice versa. These results support the concept that the volemic state of a heart can be monitored continuously in real time with temporary pace leads incorporating accelerometer sensors post-operatively. These novel accelerometer-based measurements were comparable to the current clinical standard methods, i.e. the PiCCO and the pulmonary artery catheter, both to estimate changes in preload and to identifying fluid responsiveness.

As this method can be applied using combined accelerometer and temporary pace lead, which is routinely placed on open heart surgery patients, it does not require any additional procedure. It may therefore limit the need for additional invasive equipment like PiCCO and PA-catheter. In contrary to those methods, this method does not come in contact with the blood stream directly. On the other hand, this limits the usage of the accelerometer to open heart surgery patients unless e.g. percutaneous techniques are developed. Both the accelerometer and PiCCO gives a continuous measure of hemodynamic values, however, a disadvantage of PiCCO is that it is dependent on a thermodilution calibration and will drift based on vascular compliance and must therefore be recalibrated when changes in vascular compliance occur [13]. The accuracy and precision of PiCCO will also be affected by aortic valve regurgitation and over- or under-damped arterial pressure waveforms [13]. As the accelerometer does not utilize pressure waveforms, which might be affected by external factors, but rather measure the heart wall vibrations directly, its accuracy and precision will most likely not be affected by the aforementioned conditions. However, this must be verified in future comparative studies. The pulmonary artery catheter gives an intermittent estimate of LV preload and thus limits the usefulness of this method if monitoring rapid changes in unstable patients [13]. However, this method gives measurements of filling pressures and SvO2, which the accelerometer does not.

We found that the accuracy of f_{S1} to estimate relative changes in preload was comparable to the clinical standard $GEDV_{PiCCO}$. Our study was not designed to show superiority to PiCCO in estimating EDV as the accuracy and precision of PiCCO estimates have previously been found to be adequate [14]–[17]. The accuracy may be considered relatively high in both cases as the bias for both were below 5%. The Bland-Altman analysis did show that the limits of agreement was about twice as large for $GEDV_{PiCCO}$ as for f_{S1}, which suggests that f_{S1} is comparable or may be a more robust estimation of changes in EDV.

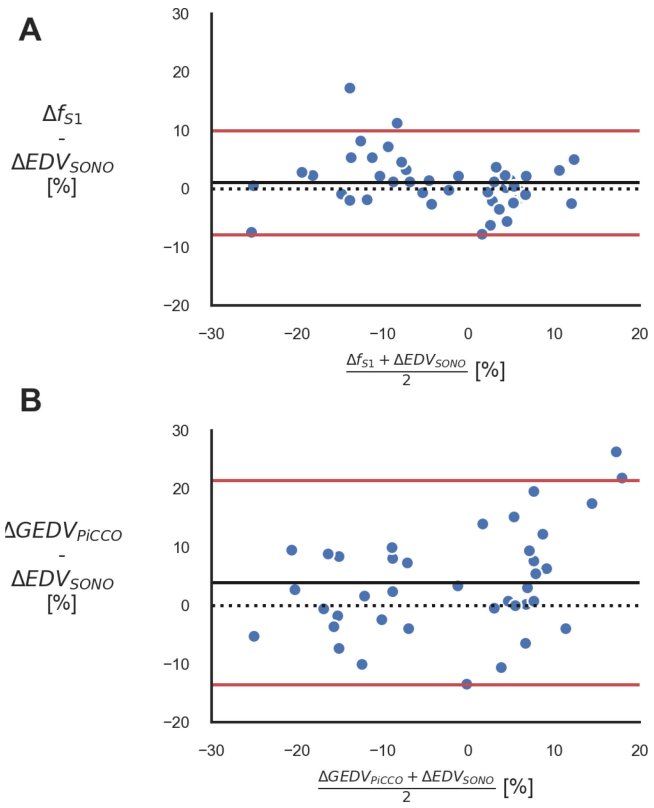

Fig. 6. Bland-Altman plots showing the agreement between A) Δf_{S1} and ΔEDV_{SONO}; and B) $\Delta GEDV_{PiCCO}$ and ΔEDV_{SONO}. The bias (1.96 SD) for Δf_{S1} was 1.0 (8.9)%. The bias (1.96 SD) for $\Delta GEDV_{PiCCO}$ was 4.0 (17.5)%. The data were pooled from all experiments. Black, solid lines signify bias, red lines signify bias $\pm$ 1.96SD. Δf_{S1}: relative change in myocardial acceleration frequency from baseline. ΔEDV_{SONO}: relative changes in end-diastolic volume measured using sonomicrometry. $\Delta GEDV_{PiCCO}$: relative changes in global end-diastolic volume, measured using PiCCO.

Combined with a measure of heart function, like peak systolic velocity [2] or pressure-displacement loop area [1], the accelerometer may be used to give a robust estimate of a patient's position on the Frank-Starling curve. This was reflected in the results of the linear regression analysis, assessing the correlation of the preload parameters to stroke volume. The average correlation among subjects between SV_{SONO} and f_{S1} was stronger than both the clinically available measures $GEDV_{PiCCO}$ and PAOP, when assessing both the individual and the pooled data. The PiCCO also showed large variation in the slopes of the individual regression lines, while the slopes for f_{S1} were more aligned, which suggests that the f_{S1} might be less susceptible to inter-subject variability.

The results in Table I showed that we successfully introduced both a state of hypovolemia and hypervolemia, with significantly decreased and increased EDV, SV and cardiac output, relative to baseline. However, we observed that the EDV did only marginally increase during infusion of saline. The reason for this might be autonomous volemic compensation resulting in increased fluid retention. Because of this we were not able to reach the state of overloading at the descending limb of the Frank-Starling curve. However, there are studies suggesting that in myocardial tissue there is not a descending limb of the Frank-Starling relation [18], [19], and that the cause of decreased heart function during overloading is due to systemic heart failure from excessive fluid. On the other hand, the topic of this study was estimation of preload and not preload induced changes in function. In the latter case, it would presumably be of more interest to apply a heart failure experimental model that also exhibited the descending limb at high preloads.

Predicting fluid responsiveness is important during fluid resuscitation of hemodynamically unstable patients. We found that the diagnostic accuracy (area under the ROC curve) for identifying fluid responsiveness using f_{S1} was comparable to SVV_{PiCCO} and PPV_{PiCCO}. The diagnostic accuracy of SVV_{PiCCO} and PPV_{PiCCO} obtained in this study was lower than in previous findings [6], [20]. However, the definition of fluid responsiveness is commonly the increase in SV after a 'fluid challenge', and there has not been an international consensus as to what defines a 'fluid challenge' [21]. Therefore, as we have defined fluid responsiveness based on changes in SV measured with sonomicrometry, the results reported in this study might not be comparable to previous findings. As this is a proof of concept study, the intention was not to report the actual diagnostic accuracy, but rather to compare the accuracy to clinically accepted methods.

Although SVV measured using PiCCO has been shown to have good diagnostic accuracy [20], it has also been shown to fail in predicting fluid responsiveness in open chest conditions [22], in patients on pressure support ventilation [23], and during pericardial effusion [24]. As the accelerometer is not dependent on mechanical ventilation, f_{S1} will presumably prevail under conditions affecting the ventilation, although pericardial effusion might have a dampening effect on the measured vibrations. However, this must be verified in future studies. Additionally, the PiCCO SVV may not be used in patients with arrhythmias, valvular disease, intracardiac shunts, peripheral vascular disease and decreased ejection fraction [20]. The accelerometer measures heart wall vibrations and will most likely not be affected by complications in the peripheral system, like peripheral vascular disease, but it is conceivable that arrhythmias and valvular diseases may affect the measurement. It is also conceivable that changes in the myocardial tissue due to for example scarring after myocardial infarction, stunned myocardium, hypertrophy, or artificial valves would alter how the proposed method estimates preload. However, acute changes in preload would likely still be detected, but this assumption should be tested in future studies.

The proposed principle that frequency depends on tension as shown in equation (1), also assumes that the size and density of the myocardium are constant, which seem reasonable as the myocardium is considered approximately incompressible [25]. The global, intracardial volume, on the other hand, will change with preload. According to the equation, increased volume should decrease frequency. However, frequency increased, suggesting that this effect was neglectable and that the changes in tension are dominant. Different hearts with different sizes will have a different baseline frequency according to equation (1), which is one of the reasons for why this method is only suitable for assessing relative changes in preload.

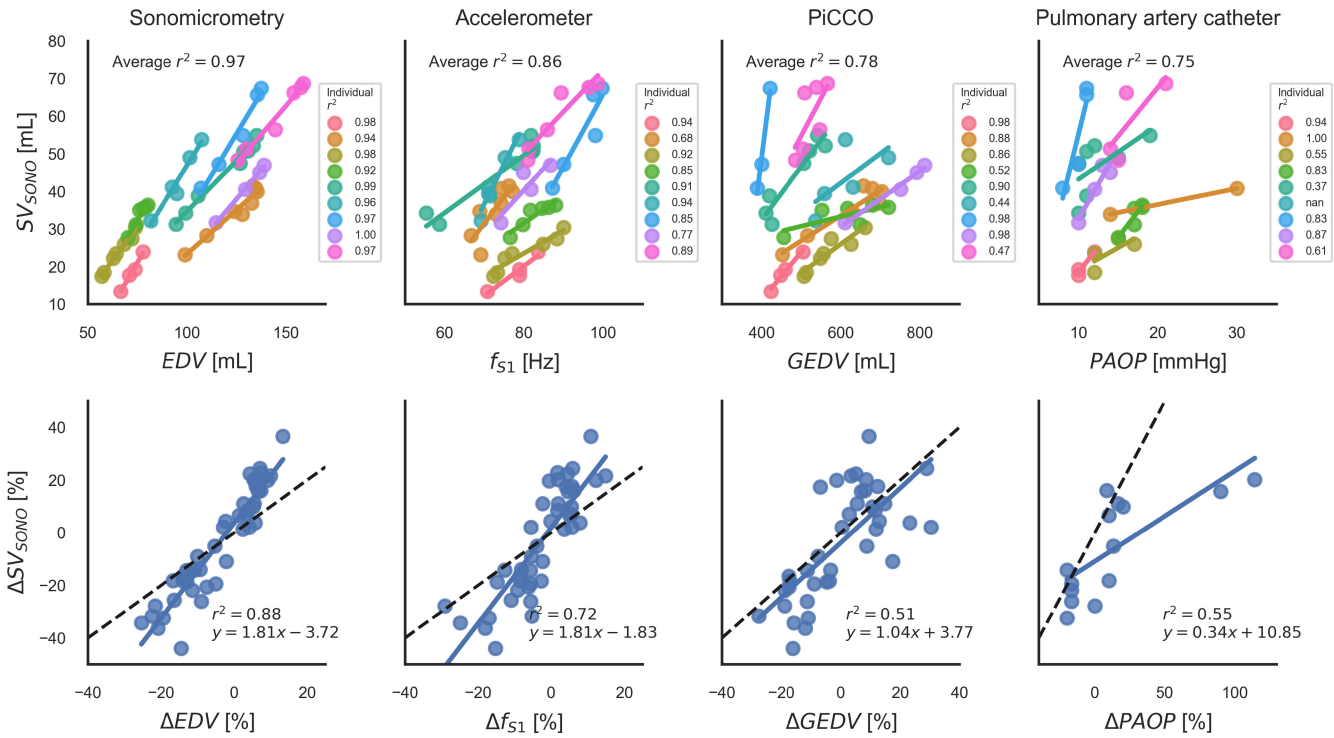

Fig. 7. Graphs showing the estimated Frank-Starling relations using the reference sonomicrometry derived stroke volume (SV_{SONO}) and end-diastolic volume (EDV), accelerometer derived index for preload (myocardial acceleration frequency (f_{S1})); PiCCO derived global EDV (GEDV), and pulmonary artery occlusion pressure (PAOP) measured using pulmonary artery catheter. The top row shows absolute values, the regression lines, and r^2, for each individual subject. The bottom row shows the relative changes in values from baseline for pooled data from all animals.

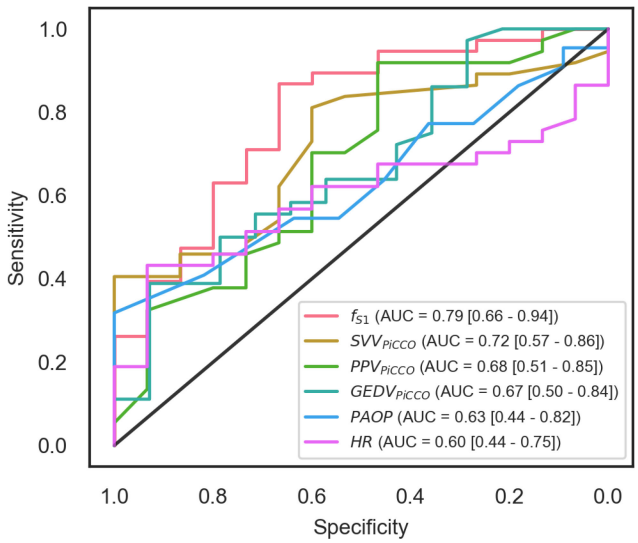

Fig. 8. Graph showing the receiver operating characteristics curves for identifying the measurements where the stroke volume variation (SVV) by sonomicrometry was above 11.6% which would indicate fluid responsiveness [6] using: myocardial acceleration frequency (f_{S1}, accelerometer), stroke volume variation (SVV, PiCCO), pulse pressure variation (PPV, PiCCO), global end-diastolic volume (GEDV, PiCCO), pulmonary artery occlusion pressure (PAOP), and heart rate (HR). The area under the curve (AUC [95% CI]) for the different predictors is also shown.

The results in this study were based on data from relatively wide hemodynamic interventions performed on healthy animals. The responses to the interventions therefore were large. In a real setting, measurements in sick patients with multiple possible comorbidities may not be as clear cut. Furthermore, the measurements were done acutely, with the animals under anesthesia, and did therefore not include the level of motion artefacts that would be presumably be present in conscious, post-operative patients. We therefore plan a clinical study with open heart surgery patients where the proposed method will be validated by echocardiography.

The results are not without limitations. In the first included experiment the unloading was performed before loading, which resulted in inability to reach a state of overloading. Consequently, the data from this animal only included unloading interventions and were therefore excluded from Table I. Another limitation was that our model did not include changes in contractility and afterload. How changes in contractility and afterload affect our proposed method should therefore be addressed in future studies. Additionally, the data were recorded using a software that was not considered hard real-time, and the uniformity of time between samples could therefore not be guaranteed. However, the pre-processing steps would ensure that variations in sampling frequency would not affect the results.

V. Conclusion

An epicardially placed accelerometer, continuously measuring heart wall vibrations, can be used to assess changes in preload in real time. This proof of concept study shows the feasibility of using epicardial pacing leads incorporating accelerometers to monitor the volemic status post-operatively, thereby guiding

fluid resuscitation and the need for inotropic support. Epicardial pacemaker wires may therefore become important tools in the management of cardiac surgery patients and minimize the complexity of monitoring. However, more studies are needed to validate the assumptions clinically.

Acknowledgment

The authors would like to thank the staff at the Intervention Centre, Oslo University Hospital for support during the animal study.

Competing Interest: EF, OJE, and PSH are patent holders of the accelerometer technology for assessing cardiac function, and are together with MRK, OJHNG, and EWR shareholders in Cardiaccs A/S which is commercially exploiting this technology. MRK has gained employment in Cardiaccs AS during this study. EF is chairman of the board at Cardiaccs AS. JB declares no competing interests.

References

[1] P. S. Halvorsen *et al.*, "Automatic real-time detection of myocardial ischemia by epicardial accelerometer," *J. Thorac. Cardiovascular Surgr.*, vol. 139, no. 4, pp. 1026–32, Apr. 2010.

[2] O.-J. H. N. Grymyr *et al.*, "Continuous monitoring of cardiac function by 3-dimensional accelerometers in a closed-chest pig model," *Interact. Cardiovascular Thorac. Surgr.*, vol. 21, no. 5 pp. 573–582, Nov. 2015.

[3] O.-J. H. N. Grymyr *et al.*, "Assessment of 3D motion increases the applicability of accelerometers for monitoring left ventricular function," *Interact. Cardiovasc. Thorac. Surg.*, vol. 20, no. 3, pp. 329–337, Mar. 2015.

[4] O. J. Elle *et al.*, "Early recognition of regional cardiac ischemia using a 3-axis accelerometer sensor," *Physiol. Meas.*, vol. 26, no. 4, pp. 429–40, Aug. 2005.

[5] P. E. Marik *et al.*, "Does central venous pressure predict fluid responsiveness?" *Chest*, vol. 134, no. 1, pp. 172–178, Jul. 2008.

[6] P. E. Marik *et al.*, "Dynamic changes in arterial waveform derived variables and fluid responsiveness in mechanically ventilated patients: A systematic review of the literature," *Crit. Care Med.*, vol. 37, no. 9, pp. 2642–2647, Sep. 2009.

[7] G. Plicchi *et al.*, "PEA I and PEA II based implantable haemodynamic monitor: Pre clinical studies in sheep," *EP Europace*, vol. 4, no. 1, pp. 49–54, Jan. 2002.

[8] J. C. Wood, A. J. Buda, and D. T. Barry, "Time-frequency transforms: A new approach to first heart sound frequency dynamics," *IEEE Trans. Biomed. Eng.*, vol. 39, no. 7, pp. 730–740, Jul. 1992.

[9] J. C. Mercier *et al.*, "Two-dimensional echocardiographic assessment of left ventricular volumes and ejection fraction in children," *Circulation*, vol. 65, no. 5, pp. 962–969, May 1982.

[10] M. R. Krogh *et al.*, "Dynamic gravity compensation does not increase detection of myocardial ischemia in combined accelerometer and gyro sensor measurements," *Sci. Rep.*, vol. 9, no. 1, pp. 1–10, Feb. 2019.

[11] "R: A language and environment for statistical computing," R Foundation for Statistical Computing, 2018. [Online]. Available: https://www.r-project.org/

[12] E. R. Delong *et al.*, "Comparing the areas under two or more correlated receiver operating characteristic curves: A nonparametric approach," *Biometrics*, vol. 44, no. 3, pp. 837–845, Sep. 1988.

[13] J. Vincent *et al.*, "Clinical review: Update on hemodynamic monitoring - A consensus of 16," *Crit. Care*, vol. 15, no. 229, pp. 1–8, Aug. 2011.

[14] C. K. Hofer *et al.*, "Volumetric preload measurement by thermodilution: A comparison with transoesophageal echocardiography," *Br. J. Anaesth.*, vol. 94, no. 6, pp. 748–755, Jun. 2005.

[15] T. Tagami *et al.*, "The precision of PiCCO measurements in hypothermic post-cardiac arrest patients," *Anaesthesia*, vol. 67, no. 3, pp. 236–243, Mar. 2012.

[16] P. E. Marik, "Noninvasive cardiac output monitors: A state-of the-art review," *J. Cardiothorac. Vasc. Anesth.*, vol. 27, no. 1, pp. 121–134, Feb. 2013.

[17] E. Litton and M. Morgan, "The PiCCO monitor: A review," *Anaesth. Intensive Care*, vol. 40, no. 3, pp. 393–409, May 2012.

[18] S. J. Sarnoff and E. Berglund, "Starling's law of the heart studied by means of simultaneous right and left ventricular function curves in the dog," *Circulation*, vol. 9, pp. 706–718, May 1954.

[19] T. D. Moore *et al.*, "Ventricular interaction and external constraint account for decreased stroke work during volume loading in CHF," *Amer. J. Physiol. Circ. Physiol.*, vol. 281, no. 6, pp. H2385–H2391, Dec. 2017.

[20] Z. Zhang *et al.*, "Accuracy of stroke volume variation in predicting fluid responsiveness: A systematic review and meta-analysis," *J. Anesth.*, vol. 25, no. 6, pp. 904–916, Dec. 2011.

[21] Z. U. Mohamed and J. W. Mullenheim, "Predicting fluid responsiveness," *Trends Anaesth. Crit. Care*, vol. 2, no. 1, pp. 15–19, Feb. 2012.

[22] E. E. C. De Waal *et al.*, "Dynamic preload indicators fail to predict fluid responsiveness in open-chest conditions," *Crit. Care Med.*, vol. 37, no. 2, pp. 510–515, Feb. 2009.

[23] A. Perner and T. Faber, "Stroke volume variation does not predict fluid responsiveness in patients with septic shock on pressure support ventilation," *Acta Anaesthesiol. Scand.*, vol. 50, no. 9, pp. 1068–1073, Oct. 2006.

[24] O. Broch *et al.*, "Dynamic variables fail to predict fluid responsiveness in an animal model with pericardial effusion," *J. Cardiothorac. Vasc. Anesth.*, vol. 30, no. 5, pp. 1205–1211, Oct. 2016.

[25] H. Ashikaga *et al.*, "Changes in regional myocardial volume during the cardiac cycle: Implications for transmural blood flow and cardiac structure," *Amer. J. Physiol. Heart Circ. Physiol*, vol. 295, no. 2, pp. H610–H618, Aug. 2008.